Fractal Nanochannels as the Basis of the Ionic Transport in AgI-Based Glasses

Piercarlo Mustarelli,* Corrado Tomasi, and Aldo Magistris

Department of Physical Chemistry "M. Rolla", University of Pavia, and IENI-CNR, Via Taramelli 16, 27100 Pavia, Italy

Received: May 4, 2005; In Final Form: July 18, 2005

We propose a new model to explain the transport properties of AgI-based fast ion conducting glasses. The main factor affecting the ionic conductivity is the mobility of the Ag^+ carriers, that is controlled by the Ag local environment. We model the ionic conductivity in terms of a percolation between a low-conducting phase (purely oxygen-coordinated sites), and a high-conducting one (iodine/oxygen, I/O, coordinated sites). The percolation takes place along pathways with fractal structure. The nature of the glass network, and namely its connectivity and dimensionality, plays a significant role only for low I/O values, originating the transport and thermal anomalies observed in borate and phosphate glasses.

Introduction

Fast ion conducting (FIC) glasses are of wide interest for their potential applications as solid electrolytes in electrochemical devices, such as sensors and smart windows. Tailoring of glasses with the required mechanical, thermal, and electrical properties does need for a deep understanding of the relationships among structure, microstructure and ionic transport. In this sense, AgI-based glasses of the family $AgI-Ag_2O-M_xO_y$ (M = B, P, Mo, As, W, etc.) are indeed a good model system, since they give a very high ionic conductivity near room temperature ($\sigma_{rt} > 10^{-2}$ ohm^{-1} cm^{-1}) [1], and also because they are easily studied by means of many experimental techniques, including impedance spectroscopy,[2−6] IR [7] and Raman[8,9] spectroscopies, NMR,[10] X-rays[11] and neutron diffraction,[12] neutron scattering,[13,14] XAS,[15,16] acoustic absorption,[17] ac conductivity,[18,19] and Brillouin scattering.[20]

Many approaches have been proposed in order to explain the transport properties of AgI-based glasses: (i) thermodynamic models, such as the weak electrolyte[21,22] and the regular solutions theory,[23] (ii) topologic/chemical ones,[24−26] and (iii) microscopic models, such as the cluster[27−29] and the cluster-bypass,[30] which imply the formation of AgI microclusters in the glass, the dynamic structure,[31−33] and the diffusion pathway model,[9,34,35] where in contrast, the dopant salt is assumed to be homogeneously distributed in the glass matrix. Microscopic interpretations of the conductivity spectra, like the jump diffusion model,[36] and the derived concept of mismatch and relaxation[37] also point to a wide distribution of the correlation times of cations dynamics, which is compatible with a quite homogeneous distribution of the cations in the glasses. Support for this picture has been recently given by 2-D NMR studies on AgI-based phosphate glasses.[38,39]

At present, it is believed that the main role of AgI is to expand the glass network and to create free volume for the ions transport.[40,41] Reverse Monte Carlo (RMC) structural models of borate and molybdate glasses, coupled with bond valence calculations, showed that the conductivity is related to the formation of "infinite pathways clusters" for transport, where the silver ions do experience mixed I/O coordination.[42−46] While the nature of the local environment, i.e., the mixed I/O coordination, of the silver cations inferred by RMC analyses has been confirmed by means of IR[35] and NMR,[47−51] the intermediate range order (IR) and connectivity of the transport pathways are still debated. Percolation thresholds for conductivity were observed near 30 mol % AgI in $AgI-AgPO_3$ glasses.[40,50,52] By means of ^{109}Ag NMR line width analysis, we showed that a dramatic increase ($\sim 10^3$) of the cations mobility takes place near 30 mol % AgI in $AgI-AgPO_3$.[50] On the other hand, Martin showed that several percolation approaches, namely effective medium (EM), site (SPT), and bond (BPT) percolation, failed in predicting the conductivity behaviors of borate and phosphate glasses.[53] Thermal anomalies were also observed for 30−40 mol % AgI in phosphate[54] and borate[55] glasses.

In this paper we present a new model, which is able to justify the ionic conductivity of AgI-based FICs simply on the basis of their stoichiometry, and without any adjustable parameter. Our model is based on ^{109}Ag NMR and conductivity data taken from the literature, and corroborated by new NMR measurements on samples tailored to investigate the composition region with I/O ≥ 0.5, where scarce information was available. Our aim is to address the following points: (i) the role of carrier concentration and mobility in determining the ionic transport; (ii) the influence of the short range (SR) and the intermediate range (IR) details (i.e., the structure of conduction pathways) on the conductivity and their relationships with the bulk anomalies observed in borate and phosphate glasses.

Results and Discussion

(a) The Role of Carrier Concentration and Mobility in Determining the Transport Properties. To address this point, we can start on the general expression for the ionic conductivity

$$\sigma_i = \sum_k q_k c_k \mu_k \qquad (1)$$

where q_k is the charge of the ionic carriers of kth type, c_k is their concentration, and μ_k is their mobility. In the case of AgI-based FICs the ionic transport number is ≥ 0.99.[1] Valuable information on silver ions mobility and concentration can be

* Corresponding author. E-mail: mustarelli@matsci.unipv.it.

10.1021/jp052305b CCC: $30.25
Published on Web 08/26/2005

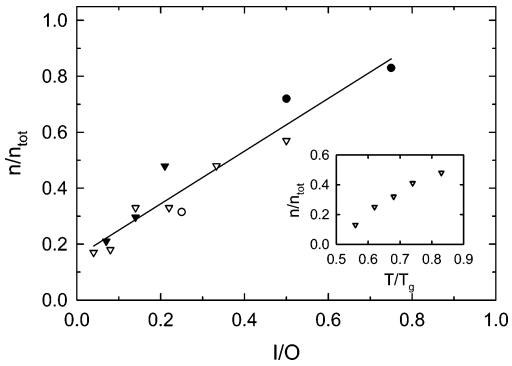

Figure 1. Fraction of Ag spins mobile in the NMR time scale, normalized to the total Ag in the glasses, vs the nominal iodines/oxygens ratio, at room temperature. Key: ▽ = AgI−$AgPO_3$ (from ref 50), ▼ = AgI−(Ag_2O·$2B_2O_3$) (from ref 51), ○ = AgI−(Ag_2O·B_2O_3) (from ref 51), and ● = AgI−Ag_2MoO_4 (unpublished data). The inset shows the same parameter vs the temperature normalized to the T_g for 0.5AgI-0.5$AgPO_3$ glass (from ref 56).

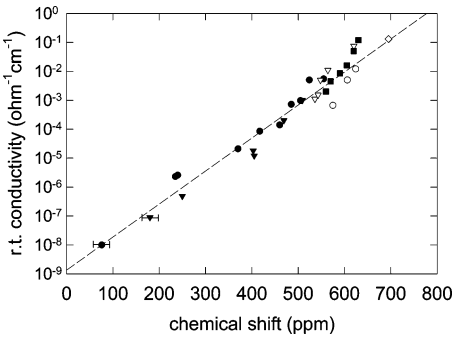

Figure 2. Ionic conductivity, σ, at room temperature vs ^{109}Ag NMR chemical shift. Key: ▽ = AgI−Ag_2O−MoO_3 (σ from refs 1, 5, and 58 (extrapolated from low temperature), NMR c.s. from refs 49 and 58), ▼ = AgI−(Ag_2O·$2B_2O_3$) (σ from ref 4, NMR c.s. from refs 47 and 51), ○ = AgI−(Ag_2O·B_2O_3) (σ from ref 4, NMR c.s. from refs 47 and 51), ● = AgI−Ag_2O−P_2O_5 (σ from refs 3, 56, and 57, NMR c.s. from refs 48 and 50), and ■ = AgI−Ag_2WO_4 (σ from ref 59, NMR c.s. from ref 59), ◇ = α-AgI (σ from ref 60 (extrapolated from high temperature), NMR c.s. from ref 61). The error bars for $AgPO_3$ and Ag_2O·$2B_2O_3$ are due to the low signal-to-noise ratio, and to chemical shift anisotropy contributions.

obtained by solid-state ^{109}Ag NMR. In fact, because of its large (∼1000 ppm) chemical shift tensor and the weak magnetic dipolar interactions ($\gamma^{109}Ag/\gamma^{1}H = 0.047$), the ^{109}Ag nucleus is well suited to study both the local environment and the single-particle correlation functions related to the ions dynamics. Solid-state NMR spectra of AgI-based glasses are typically characterized by a relatively narrow (10^1-10^3 Hz) peak assigned to the mobile nuclei, i.e., those jumping over several lattice positions in the NMR time scale (∼10^{-3} s). The chemical shift of this peak is chiefly related to the I/O ratio in the Ag^+ first coordination sphere, and a remarkable nonlinear relationship has been reported for several glass-forming systems.[51] In refs 10 and 51, we also showed that the nature of the glass former and the network dimensionality have a nonnegligible role in determining the concentration of mobile carriers at a given temperature. However, these variables account, at best, for a change of a factor ∼2 of the mobile carriers concentration.

Figure 1 shows the fraction of the mobile ions vs the nominal I/O ratio for several glassy systems. By comparing the data of Figure 1 with the results of refs 10 and 51, we can conclude that the I/O ratio (i.e., the SR) is more important that the IR details in determining the fraction of spins which are mobile at a given temperature.The effects of the temperature have been investigated in the particular case of AgI−$AgPO_3$ glasses, and estimated to be of the same magnitude of those related to the I/O ratio (see inset). Since the experimental points of Figure 1 cover adequately the glass formation regions (GFR) of several systems, on the basis of eq 1 we can state that the changes of carrier concentration will account, at best, for one order-of-magnitude change of the conductivity at room temperature. Therefore, we can conclude that the change of ions mobility is the key factor in determining the exceptionally large (up to 6 orders of magnitude) variations observed along the GFR of AgI glasses.[1−5]

(b) The Structural Parameters Controlling the Ion Mobility. Figure 2 shows the behavior of ionic conductivity at room temperature for many AgI-based glasses vs the ^{109}Ag NMR chemical shift, which is reflecting the SR structure of the glasses and, namely, the I/O ratio in the first Ag coordination sphere. In general, the points reported in figure are well distributed over the GFRs of the different systems. In particular, the points at ∼100 and ∼180 ppm refer to undoped $AgPO_3$ and $Ag_2B_4O_7$ glassy samples. The fact that many AgI-based glassy systems lie on the same line is a strong indication that long-range ions migration (which is controlled by the ions mobility, as already stated) is governed by the local environment, and therefore by the number of oxygens and iodines coordinating the cations, rather than by the intermediate range structure and connectivity of the glass network. Moreover, the presence on the line of the undoped phosphate and borate samples, which are characterized by a small but not negligible ionic conductivity, does confirm that the effort to discuss the transport properties of these glasses in terms of percolation between a true insulating and a conducting phase is destined to fail.

(c) A Model for the Conductivity. To find a unifying scenario for the AgI-based FIC glasses, we can start on the model sketched by Swenson et al.[42−46] The main assumptions of this model are as follows: (i) Ag^+ ions with a mixed oxygen/iodine coordination are the dominant species in these glasses; (ii) long-range migration pathways develop along sites where the bond-valence mismatch for the mobile ions remains below a threshold value, and the conductivity may be determined from the pathway cluster volume; (iii) although less conducting, purely oxygen-coordinated sites cannot be neglected in modeling the Ag^+ transport. Since purely oxygen-coordinated Ag^+ cannot be thought as really "immobile" (see also ref 47), we can model the ionic conductivity of AgI-based glasses as the cations percolation between a low conducting phase (purely oxygen-coordinated sites), and a high conducting one (mixed iodine−oxygen coordinated sites). The addition of AgI to the modified glassy networks $Ag_2O-M_xO_y$ will cause the progressive increase of the mixed coordination sites which, in turn, will give a continuous variation of the conductivity vs AgI content (see next paragraph), in agreement with the experimental behaviors reported in the literature (see, for example, refs 3, 4, and 55). We stress that this "graded percolation" approach is different from that proposed by Martin,[53] where the conducting phase was given by AgI microdomains, and the increase of the conductivity was due to the "co-connectivity" between the oxyanion phase and the I^- polyhedra sublattice. Whereas Martin's model does not imply chemical reactions between O- and I-based sublattices, our approach does require a chemical modification of the site occupied by the cations.

In the general frame of SPT, the ionic conductivity may be expressed as[62]

$$\sigma \propto (x - x_{cs})^{\alpha} \qquad (2)$$

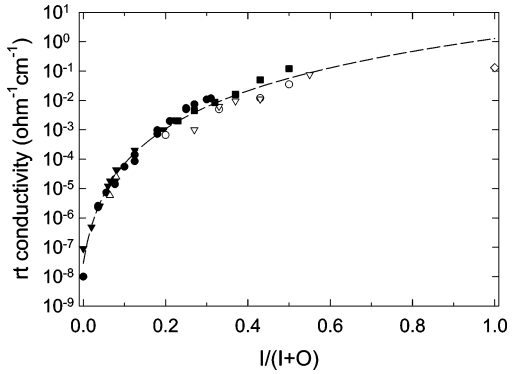

Figure 3. Ionic conductivity, σ, at room temperature vs the molar fraction of "conducting bonds", I/(I + O). Key: ▽ = AgI−Ag_2O−MoO_3 (σ from refs 1, 5, and 58 (extrapolated from low temperature), ▼ = AgI−(Ag_2O·$2B_2O_3$) (σ from ref 4), ○ = AgI−($Ag_2O.B_2O_3$) (σ from ref 4), △ = AgI−(Ag_2O·$4B_2O_3$) (σ from ref 4), ● = AgI−Ag_2O−P_2O_5 (σ from refs 3, 56, 57), ■ = AgI−Ag_2WO_4 (σ from ref 59), and ◇ = α-AgI (σ from ref 60 (extrapolated from high temperature)). The dashed line is the nonlinear best-fit with eq 2 (three parameters, Levenberg−Marquardt algorithm, $R^2 = 0.99$).

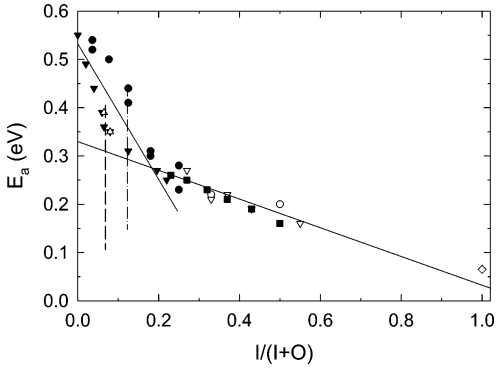

Figure 4. Activation energy for ionic conductivity vs the molar fraction of "conducting bonds", I/(I + O). Symbols and references are the same of Figure 3. The solid lines are linear regressions performed on two families of points with I/(I + O) ≥ 0.2 ($R^2 = 0.92$) and I/(I + O)<0.2 ($R^2 = 0.68$), respectively. Dashed line: step transition of the system AgI−(Ag_2O·$2B_2O_3$). Dash−dot line: step transition of the system AgI−$AgPO_3$.

where x is the molar fraction of the conducting phase, x_{cs} is the threshold value for site percolation, and α is a critical exponent that gives information about the nature and the dimensionality of the network involved in the transport process. Since the conducting nature of a site is related to the presence of I atoms in its first coordination sphere, a good expression for the molar fraction of the conducting phase is $x = I/(I + O)$, where I and O are obtained from the glasses stoichiometry. The noninsulating nature of purely O-coordinated sites, which leads to the graded increase of conductivity on AgI addition, will be likely accounted for by a value of x_{cs} near to zero. Figure 3 shows the behavior of the ionic conductivity for many systems vs the I/(I + O), fitted with eq 2. As the threshold value we obtained $x_{cs} \cong 0$. Within the limits of the best-fit method we employed (see caption of Figure 3), this value reflects the noninsulating nature of purely O-coordinated sites. As far as concerns the value of the critical exponent, we obtained $\alpha \cong 3.38$. Values of $\alpha \geq 3$ may be associated with the percolation through a fractal structure; in fact, the exact value of 3 has been obtained by solving the percolation problem through a Bethe lattice, that is a lattice of branching structures with no closed loops.[63] Percolation through a Bethe lattice was used to rationalize the gelation theory developed by Flory about the branching of small molecules in a polymerization process which leads to a gel.[64] Following our model, the progressive chemical modification of O-coordinated sites in I/O-coordinated sites, due to the addition of AgI, is resembling the polymerization process described by Flory. It is worthwhile to discuss the limits of our model at the two extremes of the compositional range. For $x \sim 0$ the less conducting phase is the dominant one, and the nature of the glass matrix (dimensionality and presence of nonbrigding oxygens) may play an important role in determining the ionic transport.[10] This point will be further addressed in the following. For low x values, moreover, also small effects of AgI on the glass matrix should be taken into account.[7] For $x \sim 0.5-0.6$, AgI clustering cannot fully be ruled out,[7] although it is not revealed by our ^{109}Ag NMR spectra of borate, phosphate, and molybdate glasses. In fact, if present, AgI clustering would cause a change of the stoichiometry of the glassy conducting phase so determining an effective upper limit for our model. On the other hand, while we have not experimental points for I/(I + O) ≥ 0.6, the extrapolation of the best-fit curve for $x = 1$ gives a conductivity a factor of 10 higher than that of α-AgI (see caption). This again suggests that the transport mechanism in AgI-based glasses is different from that of α-AgI, in agreement with the absence of AgI clusters.

Our graded percolation approach can also explain the thermal and electrical anomalies observed in borate[40,50,52] and phosphate[54] glasses. Since the addition of AgI to the oxyanion matrix leads to the progressive formation of mixed I/O sites, there will be a crossover point, depending from the coordination numbers of the Ag sites, above which each site will see, in average, at least one iodine among its first neighbors. A change of the ions transport efficiency (or even mechanism) is expected at the crossover. If we assume a value of 3.5−4 for the coordination number of the silver cations,[45,47] the crossover will fall at I/(I + O) ≅ 0.2−0.22. Figure 4 shows that the activation energy, E_a, for conductivity decreases with the increase of the molar fraction of conducting bonds. However, the E_a values of the glasses with I/(I + O) ≥ 0.2 are well fitted by a single linear regression, while the points with I/(I + O) < 0.2 are much more scattered, and the curves they lie on are dependent on the glass former. On the other hand, it was shown that the glass forming network may play an important role for low AgI content,[43] due to the nonbridging oxygens or to intermediate range structure.

The systems AgI−(Ag_2O·$2B_2O_3$) and AgI−$AgPO_3$ (▼ and ● in the figure, respectively) show E_a step transitions at I/(I + O) ≅ 0.075 and 0.125, respectively (see Caption), which correspond to 35 mol % AgI for borates, and to 30 mol % AgI for phosphates, in excellent agreement with the compositional positions of all the observed anomalies. In the frame of our SPT approach, we can take the abovementioned x values as the minimum AgI content for which completely connected clusters of O−Ag−I conduction sites are formed. The abscissas of the step transitions, as well as their ratios to the ∼0.2 limit (where all Ag sites are I/O connected), will then depend on the glassy network dimensionality, and on the exact value of the Ag coordination number in the glasses. A check of the validity of our approach may come from the comparison of the percolation thresholds we found with the percolation values of lattices with known dimensionality. A rough estimation shows that $x \cong 0.075$ obtained for the borate system (dashed line of Figure 4) corresponds to a percolation threshold, $p_{cs} \cong 0.375$, which is in good agreement with the value of ∼0.43 reported for a three-dimensional diamond network (coordination number, $Z = 4$).[62] The value $x \cong 0.125$ (dash−dot line of Figure 4) for phosphates (which are comparable to linear polymers, especially in the case of $AgPO_3$-based glasses) corresponds to $p_{cs} \cong 0.63$, which is

intermediate between the percolation thresholds of two-dimensional honeycomb ($\sim$0.70, $Z = 3$) and square ($\sim$0.59, $Z = 4$) lattices.[62]

Conclusions

In conclusion, our model allows us to account for the transport properties of AgI-based oxide glasses simply in terms of their stoichiometry and specifically in terms of the ratio I/O. Our model, which also allows to reconcile several bulk anomalies, does foresee that the ions transport takes place along nanochannels, with a fractal structure, of sites with mixed I/O coordination. The formation of nanochannels has been recently reported for silicate glasses and melts.[65] Our recent molecular dynamics experiments performed on very large samples (up to $\sim$15000 atoms) of $0.5AgI-0.5(Ag_2O{\cdot}2B_2O_3)$ glass support this picture.[66]

Experimental Details

The details of glasses preparation are reported in the cited papers. Here we will give more information about the NMR determination of the number of mobile Ag^+ carriers. ^{109}Ag solid-state NMR measurements were performed with a AMX400 WB spectrometer (9.4 T, Bruker, Karlsruhe, Germany), equipped with a wide-line probe (Bruker, Karlsruhe, Germany), at the Larmor frequency of 18.61 MHz. The spectra were referenced to a 10 M aqueous solution of $AgNO_3$. A 90° pulse of 16 μs, a repetition time varying from 100 to 500 s depending on the sample, and a bandwidth of 200 kHz were chosen. A total of 64−128 accumulations were generally enough to obtain acceptable *S*/*N* ratios. Both the glassy samples and the reference solution were kept in standard thin-wall, 10 mm glassy tubes (Bruker). The glassy samples were kept at the center of the NMR coil (19 mm length, 9.5 mm inner diameter). The spectra were obtained both by single-pulse and Hahn-echo sequences.

The quantitative estimation of the mobile silver ions was obtained by comparing the areas of their peaks ($T_1 \sim 1$ s at room temperature) with those of known volumes of $AgNO_3$ aqueous solutions with concentration in the range 1−10 M. This was made in order to check the linearity of the electronic response of the spectrometer receiver. The nonlinearity was less than 5%. Several other experimental conditions were varied to check the reliability of the quantitative analysis: (i) the solution volume was changed from 1 cm^3 (i.e., roughly the volume of the glassy samples), kept at the coil center, to 2.25 cm^3 in order to evaluate the borders distortions of the rf pulse B_1; (ii) several repetition delays for the solution ($T_1 > 1$ min) up to 25 min were compared to avoid signal saturation; (iii) a $AgNO_3$ solution with added 0.25 M $Fe(NO_3)_3$ was also prepared in order to reduce T_1 of silver; (iv) different aliquots of the same glass were measured, and the results were compared. By combining the errors evaluations obtained by these tests we estimated a maximum error of 20% in the case of spectra with a poor *S*/*N* ratio.

References and Notes

(1) See, for example: Magistris, A. In *Fast Ion Transport in Solids*; Scrosati, B., et al. Eds.; Kluwer Acad. Publ.: Dordrecht, The Netherlands, 1993; p 213 and references therein.
(2) Minami, T.; Takuma, Y.; Tanaka, M. *J. Electrochem. Soc.* **1977**, *124*, 1659.
(3) Malugani, J. P.; Wasniewski, A.; Doreau, M.; Robert, G.; Al Rikabi, A. *Mater. Res. Bull.* **1978**, *13*, 427.
(4) Chiodelli, G.; Campari Vigano, G.; Flor, G.; Magistris, A.; Villa, M. *Solid State Ionics* **1983**, *8*, 311.
(5) Kawamura, J.; Shimoji, M. *J. Non-Cryst. Solids* **1986**, *88*, 281.
(6) Grant, R. J.; Ingram, M. D.; Turner, L. D. S.; Vincent, C. A. *J. Phys. Chem.* **1978**, *82*, 2838.
(7) Kamitsos, E. I.,; Kapoutsis, J. A.; Chryssikos, G. D.; Hutchinson, J. M.; Pappin, A. J.; Ingram, M. D.; Duffy, J. A. *Phys. Chem. Glasses* **1995**, *36*, 141.
(8) Fontana, A.; Mariotto, G.; Cazzanelli, E.; Carini, G.; Cutroni, M.; Federico, M. *Phys. Lett.* **1983**, 93A, 209.
(9) Carini, G.; Cutroni, M.; Fontana, A.; Mariotto, G.; Rocca, F. *Phys. Rev. B* **1984**, *29*, 3567.
(10) Mustarelli, P.; Linati, L.; Tartara, V.; Tomasi, C.; Magistris, A. *Solid State Nucl. Magn. Reson.* **2005**, *27*, 112.
(11) Musinu, A.; Paschina, G.; Piccaluga, G.; Villa, M. *J. Chem. Phys.* **1987**, *86*, 5141.
(12) Swenson, J.; McGreevy, R. L.; Börjesson, L.; Wicks, J. D. *Solid State Ionics* **1998**, *105*, 55.
(13) Malugani, J. P.; Tachez, M.; Mercier, R.; Dianoux, A. J.; Chieux, P. *Solid State Ionics* **1987**, *23*, 189.
(14) Swenson, J.; Börjesson, L.; Howells, W. S. *J. Phys.: Condens. Matter* **1999**, *11*, 9275.
(15) Dalba, G.; Fornasini, P.; Rocca, F. J. *Non-Cryst. Solids* **1990**, *123*, 310.
(16) Rocca, F.; Kuzmin, A.; Mustarelli, P.; Tomasi, C.; Magistris, A. *Solid State Ionics* **1999**, *121*, 189.
(17) Carini, G.; Cutroni, M.; Federico, M.; Galli, G.; Tripodo, G. *Phys. Rev. B* **1984**, *30*, 7219.
(18) Roling, B.; Ingram, M. D.; Lange, M.; Funke, K. *Phys. Rev. B* **1997**, *56*, 13619.
(19) Cutroni, M.; Mandanici, A.; Piccolo, A.; Fanggao, C.; Saunders: G. A.; Mustarelli, P. *Solid State Ionics* **1996**, *90*, 167.
(20) Börjesson, L. *Phys. Rev. B* **1987**, *36*, 4600.
(21) Ravaine, D.; Souquet, J. L. *Phys. Chem. Glasses* **1977**, *18*, 27.
(22) Ravaine, D.; Souquet, J. L. *Phys. Chem. Glasses* **1978**, *19*, 115.
(23) Grande, T. *Phys. Chem. Glasses* **1997**, *38*, 327.
(24) Sidebottom, D. L. *Phys. Rev. Lett.* **1999**, *83*, 983.
(25) Sidebottom, D. L. *Phys. Rev. B* **2000**, *61*, 14507.
(26) Aniya, M. *Solid State Ionics*, **1995**, *79*, 259.
(27) Malugani, J. P.; Mercier, R. *Solid State Ionics* **1984**, *13*, 293.
(28) Fontana, A.; Rocca, F.; Fontana, M. P. *Phys. Rev. Lett.* **1987**, *58*, 503.
(29) Tachez, M. R.; Tachez, M.; Mercier, R.; Malugani, J. P.; Chieux, P. *Solid State Ionics* **1987**, *25*, 263.
(30) Ingram, M. D. *Philos. Mag. B* **1989**, *60*, 729.
(31) Maass, P.; Bunde, A.; Ingram, M. D. *Phys. Rev. Lett.* **1992**, *68*, 3064.
(32) Bunde, A.; Ingram, M. D.; Maass, P.; Ngai, K. L. *J. Non-Cryst. Solids* **1991**, *131−133*, 1109.
(33) Bunde, A.; Ingram, M. D.; Maass, P. *J. Non-Cryst. Solids* **1994**, *172−174*, 1222.
(34) Greaves, G. N. *J. Non-Cryst. Solids* **1985**, *71*, 203.
(35) Minami, T. *J. Non-Cryst. Solids* **1985**, *73*, 273.
(36) Funke, K. *Prog. Solid State Chem.* **1993**, *22*, 111.
(37) Funke, K.; Banhatti, R. D.; Bruckner, S.; Cramer, C.; Krieger, C.; Mandanici, A.; Martiny, C.; Ross, I. *Phys. Chem. Chem. Phys.* **2002**, *4*, 3155.
(38) Vogel, M.; Brinkmann, C.; Eckert, H.; Heuer, A. *Phys. Chem. Chem. Phys.* **2002**, *4*, 3237.
(39) Vogel, M.; Brinkmann, C.; Eckert, H.; Heuer, A. *Solid State Nucl. Magn. Reson.* **2002**, *22*, 344.
(40) Wicks, J. D.; Börjesson, L.; Bushnell-Wye, G.; Howells, W. S.; McGreevy, R. L. *Phys. Rev. Lett.* **1995**, *74*, 726.
(41) Swenson, J.; Börjesson, L. *Phys. Rev. Lett.* **1996**, *77*, 356.
(42) Swenson, J.; Börjesson, L.; McGreevy, R. L.; Howells, W. S. *Phys. Rev. B* **1997**, *55*, 11236.
(43) Adams, St.; Swenson, J. *Phys. Rev. B* **2000**, *63*, 054201/1.
(44) Adams, St.; Swenson, J. *Phys. Rev. Lett.* **2000**, *84*, 4144.
(45) Swenson, J.; Adams, St. *Phys. Rev. B* **2001**, *64*, 024204/1.
(46) Adams, St.; Swenson, J. *Chem. Phys. Phys. Chem.* **2002**, *4*, 3179.
(47) Villa, M.; Chiodelli, G.; Magistris, A.; Licheri, G. *J. Chem. Phys.* **1986**, *85*, 2392.
(48) Olsen, K. K.; Zwanziger, J. W. *Solid State Nucl. Magn. Reson.* **1995**, *5*, 123.
(49) Mustarelli, P.; Tomasi, C.; Quartarone, E.; Magistris, A.; Cutroni, M.; Mandanici, A. *Phys. Rev. B* **1998**, *58*, 9054.
(50) Mustarelli, P.; Tomasi, C.; Magistris, A.; Linati, L. *Phys. Rev. B* **2001**, *63*, 144203/1.
(51) Mustarelli, P.; Infante Garcia, M. P.; Magistris, A.; Linati, L. *Phys. Chem. Glasses* **2003**, *44*, 159.
(52) Mangion, M.; Johari, G. P. *Phys. Rev. B* **1987**, *36*, 8845.
(53) Martin, S. W. *Solid State Ionics* **1992**, *51*, 19.
(54) Tomasi, C.; Mustarelli, P.; Magistris, A.; Infante Garcia, M. P. *J. Non-Cryst. Solids* **2001**, *293*, 785.
(55) Tomasi, C. Ph.D. Thesis, University of Pavia, Italy, 2001.
(56) Tomasi, C.; Mustarelli, P.; Infante Garcia, M. P.; Magistris, A.; Mandanici, A. *Philos. Mag. B* **2002**, *82*, 475.

(57) Schiraldi, A.; Pezzati, E.; Baldini, P. *Phys. Chem. Glasses* **1986**, *27*, 190.
(58) Kuwata, N.; Saito, T.; Tatsumisago, M.; Minami, T.; Kawamura, J. *J. Non-Cryst. Solids* **2003**, *324*, 79.
(59) Hosono, M.; Kawamura, J.; Itoigawa, H.; Kuwata, N.; Kamiyama, T.; Nakamura, Y. *J. Non-Cryst. Solids* **1999**, *244*, 81.
(60) Angell, C. A. *Solid State Ionics* **1986**, *18&19*, 72.
(61) Kuwata, N.; Kawamura, J.; Nakamura, Y.; Okuda, K.; Tatsumisago, M.; Minami, T. *Solid State Ionics* **2000**, *136*−*137*, 1061.
(62) Sahimi, M. *Applications of Percolation Theory*; Taylor & Francis: London, 1994.
(63) Stauffer, D.; Aharony, A. *Introduction to Percolation Theory*, 2nd ed.; Taylor & Francis: London, 1994.
(64) Flory, P. J. *J. Am. Chem. Soc.* **1941**, *63*, 3083.
(65) Meyer, A.; Horbach, J.; Kob, W.; Kargl, F.; Schoeber, H. *Phys. Rev. Lett.* **2004**, *93*, 27801/1.
(66) Infante Garcia, M. P.; Mustarelli, P.; Tomasi, C.; Magistris, A. Manuscript in preparation.